874. The squeeze film effect on micro-electromechanical resonators

Shih-Chieh Sun[1], Chi-Wei Chung[2], Chao-Ming Hsu[3], Jao-Hwa Kuang[4]
[1, 2, 4]Department of Mechanical and Electromechanical Engineering
National Sun Yat-Sen University, Taiwan, R. O. C.
[3]Department of Mechanical Engineering
National Kaohsiung University of Applied Sciences, Taiwan, R. O. C.
E-mail: [1]*d943020006@student.nsysu.edu.tw*, [2]*ymmc_3@msn.com.tw*,
[3]*jammy@cc.kuas.edu.tw*, [4]*kuang@faculty.nsysu.edu.tw*

(Received 28 June 2012; accepted 4 December 2012)

Abstract. The air squeeze film damping effect on the dynamic responses of clamped micro-electromechanical resonators is investigated in this study. A dynamic model for a clamped micro-electromechanical resonator with the damping consideration is derived using Lagrange's equation. The corresponding resonator eigen solutions are formulated and solved by employing the assumed-mode method. The effect of different parameters; i.e. the resonator size, ambient temperature and pressure on the squeeze film damping characteristics were simulated and investigated. The results indicate that the squeeze film damping effect may significantly affect the dynamic responses of micro-scale electromechanical resonator.

Keywords: resonators, damping effect, quality factor, assumed mode method.

Introduction

Micro-electro-mechanical resonators [1-2] have been widely used as sensors in various applications. A micro-scale poly-crystalline silicon beam type resonator was proposed by Stemme [3]. The effect of different size parameters on the resonant frequencies was measured and studied. Zook et al. [4] and Tilmans et al. [5] designed different micro-polysilicon-resonators to replace the conventional silicon piezoresistors in precision sensor applications. Legtenberg et al. [6] studied the nonlinear pull-in behavior of electrodes. Zurn et al. [7] compared the difference in dynamic response simulated from the ANSYS finite element method and measured using AFM.

The damping effect introduced from air molecules in nano- or micro scale beams were investigated by Kádá et al. [8]. The Q-factor was proposed to indicate the degree of this damping effect in low vacuum. Hosaka et al. [9-11] were used the Navier-stokes and Reynolds equations to calculate and illustrate these damping characteristics and the corresponding dynamic performance. Li [12] illustrated that the damping effect in micro beam vibration is introduced from the impact velocity variation of molecules on both sides of a micro-beam. Abdel-Rahman et al. [13] presented a nonlinear model of electrically actuated micro-beams accounting for the electrostatic force of the air gap capacitor. An energy transfer mechanism was proposed by Bao et al. [14] instead of the momentum transfer mechanism in Christian's model for microstructures air damping in low vacuum. Chen and Kuo [15] introduced squeeze damping and viscous damping effects into the micro-electrostatic comb drive; and found the gap distance extension between the oscillating and fixed electrodes may significantly reduce the damping. Hutcherson and Ye [16] investigated air damping on oscillating structures in the free-molecule regime. Kwak [17] provided admissible functions to approximate the dynamic characteristics of slewing beams.

The micro resonator is surrounded with gas. A squeeze film effect leads to a damping model and changes the resonator natural frequencies at different ambient pressures. The scale of the beams may cause the air squeeze damping effect to dominate the beam dynamic behavior.

Various continuum damping models [18-20] have been proposed in last decade. However, these models were all unsuitable for micro-systems at low vacuum. To overcome this difficulty, Bao et al. [14] provided an energy transfer model to describe the air damping effect on MEMs at low pressure.

This study investigates a plate driven by an alternating electrostatic force as shown in Fig. 1. The residual vibration of micro-electromechanical resonator is usually vibrated at its lowest resonant frequency which is dependent upon the squeeze film damping effect between electrodes. This damping effect is introduced from free molecular moment [21] and energy transfer models [14] at low vacuum. The parameter effects, i.e. beam size, ambient temperature, ambient pressure and gap distance, on the damping effect are studied.

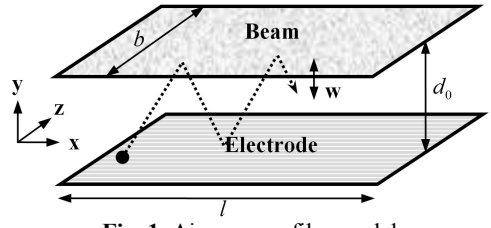

Fig. 1. Air squeeze film model

Simulation Method

The air squeeze damping effect introduced from the molecular interaction motion between a micro-scale beam type plate and electrostatic plate at low vacuum is simulated. Bao's Energy transfer model [14] is employed in this work to calculate the damping factor.

Energy transfer model [14]. The air squeeze damping effect between a clamped micro-beam and micro-electromechanical resonator electrostatic plate at low vacuum is studied in this research. The model is shown in Fig. 1. The gap distance between the micro-beam and electrostatic plate is d_0. Six admissible modes with a driving frequency of ω_e are utilized to approximate the dynamic response of the excited beam:

$$w(x,t) = A_0 \sum_{n=1}^{6} u_n(x) \sin(\omega_e t) \tag{1}$$

where A_0 is the amplitude of the micro-beam as shown in Fig. 2.

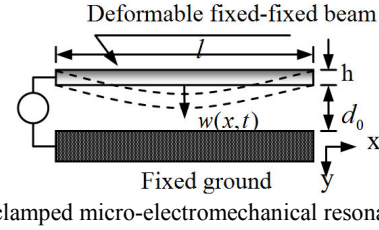

Fig. 2. The clamped micro-electromechanical resonator schematic

The energy loss from the micro-beam in the energy transfer model at low vacuum in an oscillation cycle can be approximated as:

$$\Delta W_{cycle} = \frac{lb\omega_e A_0^2 L\pi p}{4\pi d_0} \sqrt{\frac{2M_m}{\pi RT}} \sum_{i=1}^{6} \sum_{j=1}^{6} \int_0^l u_i(x) u_j(x) dx \tag{2}$$

here l, b, L are the length, width and circumference, respectively; and p, T are the sourrounding ambient pressure and absolute temperature; M_m is the mole of gas molecules; R is the gas constant in ideal gas equation; u_i and u_j are the i^{th} and j^{th} modes of vibration. The Knudsen number (Kn) is defined as the mean free path ratio of gas molecules over the characteristic length of the structure:

$$Kn = \frac{\lambda}{L_c} \tag{3}$$

For micro-electromechanical resonator with a gap distance of 1 μm and operated at a pressure of 10 torr, the Kn is 5.1. The air status in this case can be considered in the transition regime. Therefore, the intermolecular collision effect can be neglected and the air molecule collisions with resonator dominate. For simplicity the collisions between gas molecules and the resonant beam are assumed to be perfect elastic collision. In other words, the collisions between the molecules and the vibrating beam maintain the conservation linear momentum and kinetic energy laws.

The viscous damping model is employed in this study, e.g. the damping force is defined as $f_D = C_0 \partial w / \partial t$, and where C_0 is the damping factor. The energy loss in a micro-beam in oscillation introduced from the air damping is:

$$\Delta W_{cycle} = \omega_e A_0^2 \pi C_0 \sum_{i=1}^{6} \sum_{j=1}^{6} \int_0^l u_i(x) u_j(x) dx \tag{4}$$

From Eqs. (2) and (4), the damping factor (C_0) can be derived as:

$$C_0 = \frac{lbLp}{4\pi d_0} \sqrt{\frac{2M_m}{\pi RT}} \tag{5}$$

Equation (5) indicates that the damping factor is dependent upon the ambient temperature, pressure and micro-beam size and etc. This damping factor may significantly affect the dynamic responses of the small scale resonator.

Equation of damped micro-resonator. The equation of motion for the beam type micro-resonator is:

$$EI \frac{\partial^4 w}{\partial x^4} + \rho_b bh \frac{\partial^2 w}{\partial t^2} + C_0 \frac{\partial w}{\partial t} + T_a \frac{\partial^2 w}{\partial x^2} = 0 \tag{6}$$

where ρ_b is the density of resonator, and T_a is the axial force of micro-resonator. By applying the assumed-mode method, the discrete equation of motion for the micro-resonator can be derived in matrix with employing Lagrange's equation:

$$\left[M^*\right]\{\ddot{q}\} + \left[C^*\right]\{\dot{q}\} + \left[K^*\right]\{q\} = 0 \tag{7}$$

where $\left[M^*\right]$, $\left[C^*\right]$ and $\left[K^*\right]$ are the corresponding mass, damping and stiffness matrices, respectively. From the simulated eigen solutions of Eq. (7), i.e., the natural frequencies, damping ratios and normalized modes, the corresponding frequency response $H(\omega)$ can be derived as:

$$\left|H_{sr}(\omega)\right| = \frac{\left|u_i u_i^T\right|_{sr}}{2\zeta_i \omega_i^2} \tag{8}$$

Fig. 3 shows the natural frequencies of the clamped micro-resonator (without considering the air squeeze effect and the axial force effects) simulated from the finite element, the proposed methods and measured by Zook [14]. The length, width and thickness of this micro-plate are 200 μm, 45 μm and 2 μm respectively. Numerical results indicate a maximum of 15 % error was observed for the lowest few natural frequencies.

Figure 3 shows the natural frequencies of the clamped micro-resonator (without considering the air squeeze effect and the axial force effects) simulated from the finite element, the proposed methods and measured by Zook [14]. The length, width and thickness of this micro-plate are 200 μm, 45 μm and 2 μm respectively. The numerical results indicate a maximum of 15 % error was observed for the lowest few natural frequencies.

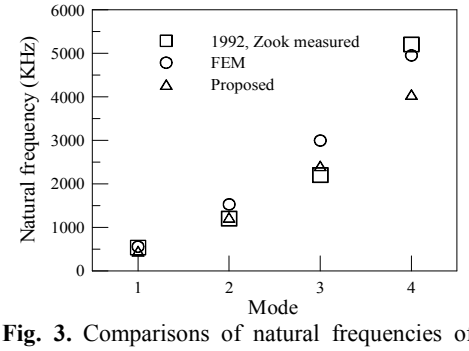

Fig. 3. Comparisons of natural frequencies of clamped micro-resonator simulated in FEM, proposed theory and measured by Zook [4]

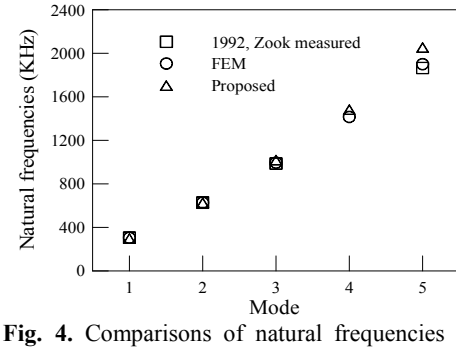

Fig. 4. Comparisons of natural frequencies in FEM, proposed theory and Zook [4] measured when there is 782.6 dyne tension force on the micro-beam resonator

However, these errors can be significantly improved by including the air squeeze and axial load effects in the dynamic model. Figure 4 shows the results for the same clamped micro-resonator considering the air squeeze damping and the axial loading effects. The errors for the simulated lowest four natural frequencies are all less than 3.2 %.

Results and discussion

As mentioned previously, the air squeeze damping may affect significantly the dynamic response in the micro- or nano-scale resonator. However, the damping effect in this clamped micro- resonator may be dependent on a few parameters, e.g. the gap distance, the ambient pressure and the ambient temperature. The damping ratio (ζ) and the Quality factor (Q-factor) for this micro-resonator are approximated by applying the half-power method on the simulated frequency response function (FRF) curves. The variation in damping ratio and Q-factor values on four major parameters are simulated and discussed below.

Gap distance. By ignoring the edge effect the electrostatic force for a micro- resonator with a driving voltage can be approximated as $\varepsilon AV^2 / 2w(x)^2$. The A, ε and $w(x)$ are the electrostatic plate area, the dielectric constant of the air and beam deformation, respectively. The variation in air squeeze film damping ratio with the initial gap distance d_0 is shown in Fig. 5 with the ambient temperature T = 27 °C and the pressure p = 1 torr and the silicon micro-beam size as $200 \times 45 \times 2$ μm. The modal damping ratios for the lowest four modes are shown in Figure 5.

The results indicate that the damping effect introduced from the squeeze air is quite significant as the initial gap distance d_0 is less than 0.7 μm.

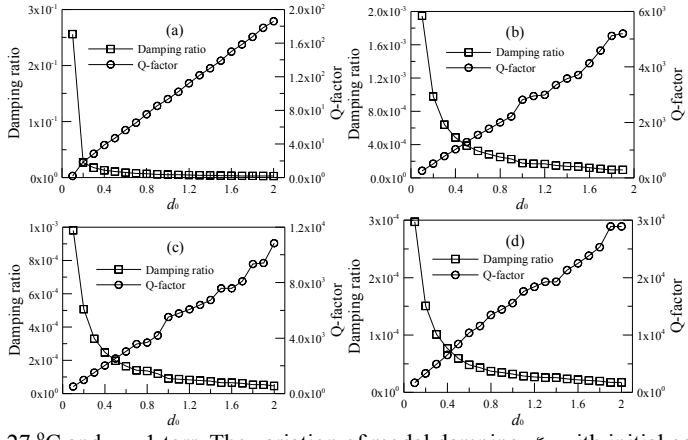

Fig. 5. At T = 27 °C and p = 1 torr. The variation of modal damping ζ_i with initial gap distance d_0:
(a) for the first mode i = 1; (b) for the second mode i = 2;
(c) for the third mode i = 3; (d) for the fourth mode i = 4

Ambient Pressure. The ambient pressure effect on the air squeeze damping is simulated and illustrated in Figure 6. The results are simulated with the ambient temperature (T) is 27 °C, and the initial gap distance d_0 is 1. The micro-beam size is $200 \times 45 \times 2$ μm. The simulated results indicate that the modal damping ratios for the lowest four modes are increased with the ambient pressure for this micro-resonator. However, the damping ratio values of the top four resonant frequencies are smaller than 10^{-4} when the pressure is less than 0.1 torr. The numerical results also indicate that the air squeeze damping effect is very sensitive to ambient pressure between 1 torr and 10 torr. This results from the increase in the number of air molecule collisions in the proposed model.

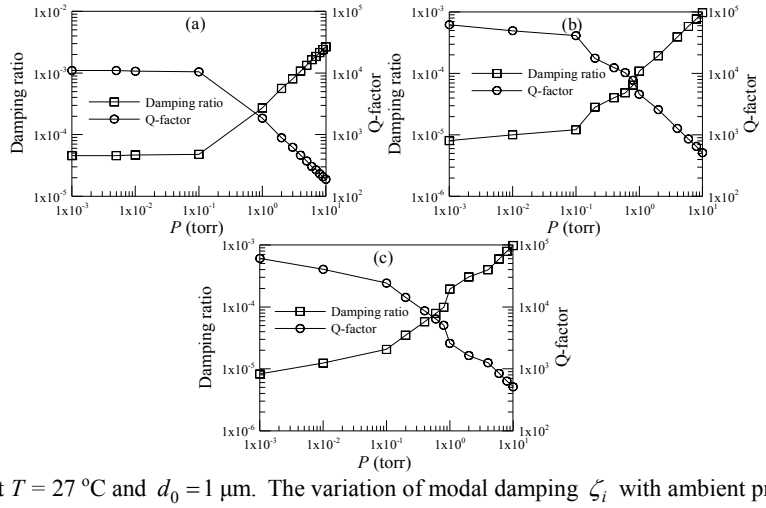

Fig. 6. At T = 27 °C and $d_0 = 1$ μm. The variation of modal damping ζ_i with ambient pressure p:
(a) for the first mode i = 1; (b) for the second mode i = 2;
(c) for the third mode i = 3; (d) for the fourth mode i = 4

Ambient Temperature. Similarly, the ambient temperature effect on the air squeeze damping ratio is simulated and discussed in Figure 7 with p = 1 torr, $d_0 = 1$ μm. The change in ambient temperature may also induce thermal stress in the axial direction to alter the natural frequencies of the silicon beam system. This thermal loading effect was also included in the proposed model. The simulated results in Fig. 7 indicate that the modal damping value rises with the temperature. The increase in damping is introduced from the increase in air molecular velocity leading to an increase in the number of collisions per unit time. Increasing the number of air molecule collisions will consume the kinetic energy of the micro-beam. However, the numerical results reveal that the ambient temperature influence is not as sensitive as the effects introduced from the gap size and the ambient pressure.

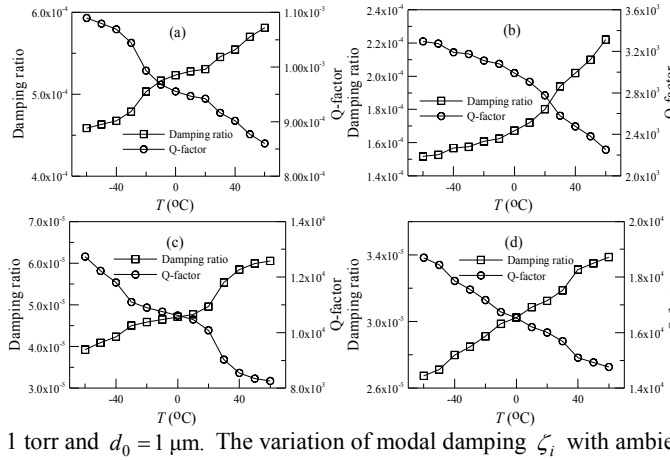

Fig. 7. At p = 1 torr and $d_0 = 1$ μm. The variation of modal damping ζ_i with ambient temperature:
(a) for the first mode i = 1; (b) for the second mode i = 2;
(c) for the third mode i = 3; (d) for the fourth mode i = 4

Micro-beam size. Equations (5) and (6) indicate that the size parameters may affect the damping ratio and the natural frequencies of the micro-resonator system. To focus on the damping subject, two size parameters, i.e. the length and width of this micro-resonator system are analyzed. The parameter 'thickness' which does not affect the contact area is not discussed in this section. Figure 8 shows the variation in the modal damping with different beam lengths based on the beam width $b = 45$ μm and the gap distance $d_0 = 1$ μm. Simulated results indicate that the modal damping ratios increase suddenly as the micro-beam length becomes larger than $l = 500$ μm. The increase in damping effect results from the increase in contact area and the resulting increase in molecular collision. However, a beam length less than 500 μm may also induce a significant damping effect increase with the decrease in beam length. This increase is induced from the rapid increase in micro-beam natural frequencies.

Similarly, the beam width effects on the modal damping ratios for a silicon micro-beam with a beam length $l = 200$ μm were simulated and shown in Figure 9. The simulation results reveal that the damping ratios increase with the beam width.

© VIBROENGINEERING. JOURNAL OF VIBROENGINEERING. DECEMBER 2012. VOLUME 14, ISSUE 4. ISSN 1392-8716

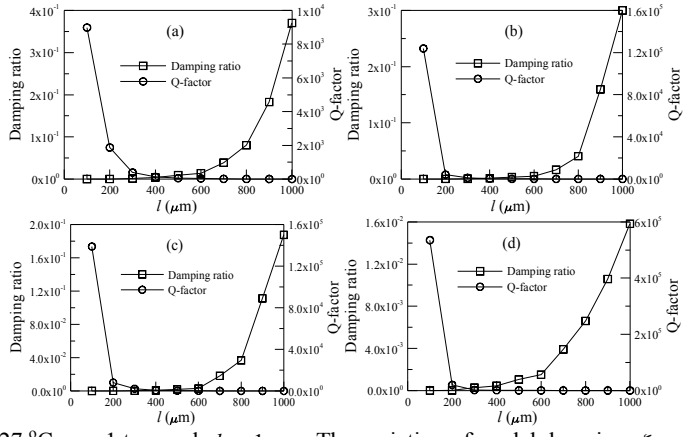

Fig. 8. At T = 27 °C, p = 1 torr and $d_0 = 1$ μm. The variation of modal damping ζ_i with micro-beam length: (a) for the first mode i = 1; (b) for the second mode i =2; (c) for the third mode i = 3; (d) for the fourth mode i = 4

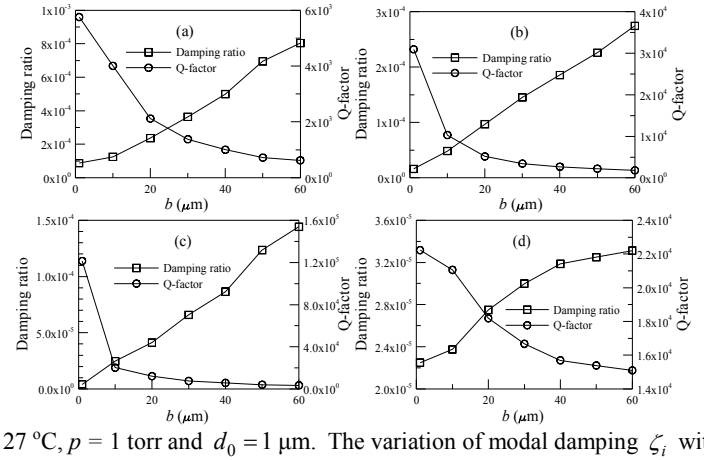

Fig. 9. At T = 27 °C, p = 1 torr and $d_0 = 1$ μm. The variation of modal damping ζ_i with micro-beam width: (a) for the first mode i = 1; (b) for the second mode i = 2; (c) for the third mode i = 3; (d) for the fourth mode i = 4

Conclusions

A molecular energy transfer model was employed to evaluate the air squeeze damping effect on the dynamic responses of a micro-scale silicon electromechanical resonator. A comparison between the simulated and measured results indicates that the proposed model is feasible for illustrating and analyzing the air squeeze damping in micro-scale beam vibration in the low vacuum case. The possible damping parameter effects, i.e. gap distance, ambient pressure, ambient temperature and micro-beam size on the variation in modal damping ratios were also investigated and discussed in this work. The results indicate that the air squeeze damping is quite sensitive to these parameters in different parameter regions. This work includes both modeling and experimental results, and validation of the modeling results with the data is emphasized.

References

[1] **Sniegowski J. J., Guckel H., Christensen T. R.** Performance characteristics of second generation polysilicon resonating beam force transducer. IEEE Solid State Sensor and Actuator Workshop, 1990, p. 9-12.

[2] **Zook J. D., Burns D. W., Guekel H., Sniegowski J. J., Englestad R. I., Feng Z.** Resonant microbeam strain transducers. Tech. Digest, 6th Int. Conf. Solid-State Sensors and Actuators, 1991, p. 664-667.

[3] **Stemme G.** Resonant silicon sensors. Journal of Micromechanics and Microengineering, Vol. 1, Issue 2, 1991, p. 113-125.

[4] **Zook J. D., Burns D. W.** Characteristics of polysilicon resonant microbeams. Sensors and Actuators A: Physical, Vol. 35, Issue 1, 1992, p. 51-59.

[5] **Tilmans H. A. C., Legtenberg R., Schurer H., Iinterma D. J., Elwenspoek M., Fluitman J. H. J.** Electro-mechanical characteristics of encapsulated driven vacuum encapsulated polysilicon resonators. IEEE Transactions on Ultrasonics, Ferroelectrics and Frequency Control, Vol. 41, Issue 1, 1994, p. 4-6.

[6] **Legtenberg R., Gilbert J., Senturia S. D., Elwenspoek M.** Electrostatic curved electrode actuators. Journal of Microelectromechanical Systems, Vol. 6, Issue 3, 1997, p. 257-265.

[7] **Zurn S., Hsieh M., Smith G., Markus D., Zang M., Hughes G., Nam Y., Arik M., Polla D.** Fabrication and structural characterization of a resonant frequency PZT microcantilever. Smart Materials and Structures, Vol. 10, No. 2, 2001, p. 252-263.

[8] **Kádár Z., Kimdt W., Bossche A., Mollinger J.** Calculation of the quality factor of torsional resonators in the low-pressure region. The 8th international Conference on Solid-State Sensors and Actuators, and Eurosensors IX, Vol. 2, 1995, p. 29-32.

[9] **Hosaka H., Itao K., Kuroda S.** Evaluation of energy dissipation mechanisms in vibrational microactuators. IEEE Workshop on Micro Electro Mechanical Systems, MEMS '94, Proceedings, 1994, p. 193-198.

[10] **Hosaka H., Itao K., Kuroda S.** Damping characteristics of beam-shaped micro-oscillators. Sensors and Actuators A: Physical, Vol. 49, Issue 1-2, 1995, p. 87.

[11] **Hosaka H., Itao K.** Coupled vibration of microcantilever array induced by airflow force. Journal of Vibration and Acoustics, Vol. 124, Issue 1, 2002, p. 26.

[12] **Li B., Wu H., Zhu C., Liu J.** The theoretical analysis on damping characteristics of resonant microbeam in vacuum. Sensors and Actuators A: Physical, Vol. 77, No. 3, 1999, p. 191.

[13] **Abdel-Rahman E. M., Younis M. I., Nayfeh A. H.** Characterization of the mechanical behavior of an electrically actuated microbeam. Journal of Micromechanics and Microengineering, Vol. 12, No. 6, 2002, p. 759.

[14] **Bao M., Yang H., Yin H., Sun Y.** Energy transfer model for squeeze-film air damping in low vacuum. Journal of Micromechanics and Microengineering, Vol. 12, No. 3, 2002, p. 341.

[15] **Chen C. S., Kuo W. J.** Squeeze and viscous dampings in micro electrostatic comb drives. Sensors and Actuators A: Physical, Vol. 107, Issue 2, 2003, p. 193.

[16] **Hutcherson S., Ye W.** On the squeeze-film damping of micro-resonators in the free-molecule regime. Journal of Micromechanics and Microengineering, Vol. 14, No. 12, 2004, p. 1726.

[17] **Kwak M. K.** New admissible functions for the dynamic analysis of a slewing flexible beam. Journal of Sound and Vibration, Vol. 210, Issue 5, 1998, p. 581.

[18] **Cho Y. H., Pisano A. P., Howe R. T.** Viscous damping model for laterally oscillating microstructures. Journal of Microelectromechanical Systems, Vol. 3, Issue 2, 1994, p. 81.

[19] **Ye W., Wang X., Hemmert W., Freeman D., White J.** Air damping in laterally oscillating microresonators: a numerical and experimental study. Journal of Microelectromechanical Systems, Vol. 12, Issue 5, 2003, p. 557.

[20] **Veijola T., Turowski M.** Compact damping models for laterally moving microstructures with gas-rarefaction effects. Journal of Microelectromechanical Systems, Vol. 10, Issue 2, 2001, p. 263.

[21] **Christian R. G.** The theory of oscillating-vane vacuum gauges. Vacuum, Vol. 16, Issue 4, 1966, p. 175.